

Fırat Üniversitesi Deneysel ve Hesaplamalı Mühendislik Dergisi



Dikdörtgen Pencerelere Sahip 3B-Baskılı Ince Cidarlı Kare Tüplerin Yarı-Statik Basma Yüklemesi Altındaki Çarpışma Dayanımı Özellikleri



¹Makine Mühendisliği Bölümü, Mühendislik ve Doğa Bilimleri Fakültesi, Hitit Üniversitesi, Çorum, Türkiye.

¹mervetunay@hitit.edu.tr

Geliş Tarihi: 30.05.2025

Walter Tarihi: 25.08.2025

Düzeltme Tarihi: 25.08.2025

doi: https://doi.org/10.62520/fujece.1709924

Kabul Tarihi: 01.10.2025 Duzeitme Tarihi:25.08.2025 Araştırma Makalesi

Alıntı: M. Tunay, '' Dikdörtgen pencerelere sahip 3b-baskılı ınce cidarlı kare tüplerin yarı-statik basma yüklemesi altındaki çarpışma dayanımı özellikleri'', Fırat Üni. Deny. ve Hes. Müh. Derg., vol. 4, no 3, pp. 701-714, Ekim 2025.

Öz

Bu çalışma, 3B baskı teknolojisi kullanılarak polilaktik asitten (PLA) üretilen ve pencereler içeren ince cidarlı kare tüplerin enerji sönümleme ve çarpışma dayanımı özelliklerini analiz etmek amacıyla tasarlanmıştır. Bunu başarmak için, tüplerin analizinde her biri iki seviyeli üç bağımsız tasarım parametresi dikkate alınmıştır: pencere sayısı (4, 5), pencere uzunluğu (8, 10 mm) ve pencere genişliği (10, 12 mm). Enerji sönümleme ve çarpışma dayanımı özelliklerini belirlemek amacıyla pencereli ince cidarlı kare tüpler yarı-statik eksenel basma testine tabi tutulmuştur. Tüplerin eksenel basması sırasında kuvvet ve ortaya çıkan yer değiştirme tepkileri kaydedilmiştir. Enerji sönümleme ve çarpışma dayanımı performansı, toplam sönümlenen enerji (EA), tepe çarpışma kuvveti (PCF), özgül enerji sönümü (SEA), ortalama ezilme kuvveti (MCF) ve çarpışma kuvveti verimliliği (CFE) gibi çeşitli kritik göstergeler ölçülerek nicelendirilmiştir. Deneysel sonuçlar, pencere boyutundaki bir artışın hem enerji sönümlemesinde hem de çarpışma kuvveti verimliliğinde bir düşüşe yol açtığını ortaya koymuştur. Örneğin, deneysel bulgular, 4W-1 numunesinin yaklaşık %18 ve %70 oranında sırasıyla 4W-2 ve 4W-3 numuneleri için kaydedilen SEA değerlerinden daha üstün bir SEA değeri sergilediğini göstermektedir. Ayrıca, 4W-1, 4W-2 ve 4W-3 numunelerinin sergilediği CFE'nin, sırasıyla yaklaşık %13, %6 ve %4'lük artışlarla 5W-1, 5W-2 ve 5W-3 numunelerinden önemli ölçüde daha yüksek olduğu görülmüştür.

Anahtar kelimeler: Pencereli ince cidarlı tüpler, 3B baskı, Çarpışma, Enerji sönümü, Ergitilmiş yığma modelleme

_

^{*}Yazışılan yazar



Firat University Journal of Experimental And Computational Engineering



Crashworthiness Characteristics Of 3D Printed Thin-Walled Square Tubes With Rectangular Holes Under Quasi-Static Compression Loading



¹Department of Mechanical Engineering, Faculty of Engineering and Natural Sciences, Hitit University, Corum, Türkiye.

¹mervetunay@hitit.edu.tr

Received: 30.05.2025 Accepted:01.10.2025 Revision:25.08.2025 doi: https://doi.org/10.62520/fujece.1709924

Research Article

Citation: M. Tunay, "Crashworthiness characteristics of 3d printed thin-walled square tubes with rectangular holes under quasi-static compression loading", Firat Univ. Jour. of Exper. and Comp. Eng., vol. 4, no 3, pp. 701-714, October 2025.

Abstract

This paper is designed to examine the crash performance and energy absorption of thin-walled windowed square tubes with incorporated windows, produced from polylactic acid (PLA) using 3D printing technology. Three independent design variables, each with two levels, were considered in the analysis of the tubes: the number of windows (4, 5), window length (8, 10 mm), and window width (10, 12 mm). To decide the absorbed energy and crash behaviors, the windowed square tubes were loaded under quasi-static compression. The force and resulting displacement responses during the axial compression of the tubes were recorded. Energy absorption and crashworthiness performance were quantified by measuring several critical indicators, including peak crash force (PCF), energy absorption (EA), specific energy absorption (SEA), mean crushing force (MCF), and crash force efficiency (CFE). The findings indicated that an increase in window size resulted in a reduction in both EA and CFE. For instance, the experimental findings illustrate that the 4W-1 specimen exhibited a SEA value that was approximately 18% and 70% superior to the SEA values recorded for the 4W-2 and 4W-3 specimens, respectively. Furthermore, The CFE demonstrated by specimens 4W-1, 4W-2, and 4W-3 considerably exceeded that of specimens 5W-1, 5W-2, and 5W-3, with percentage increases of approximately 13%, 6%, and 4%, respectively.

Keywords: Windowed thin-walled tubes, 3D printing, Crashworthiness, Energy absorption, Fused deposition modelling

_

^{*}Corresponding author

1. Introduction

Thin-walled tubes, due to their energy-absorbing capabilities, have found widespread application in the design of many vehicles, including trains, automobiles, ships, and aircraft [1-4]. In the event of a real crash, energy-absorbing structures undergo plastic deformation, gradually dissipating the crash energy and distributing the kinetic energy [5-6]. Thus, they reduce the impact effect, ensuring passenger safety and well-being, and minimizing vehicle damage. Most energy-absorbing structures are single-use, being discarded and replaced once plastically deformed. Therefore, in the design of energy-absorbing structures, it is important to select structures with low mass, low initial peak force (PCF), high specific energy absorption (SEA), and high crash force efficiency (CFE) [7-9].

In the design of energy-absorbing thin-walled tubes, a wide variety of options are available, such as tapered, windowed, corrugated, functionally graded, actuated, and origami structures, with various cross-sectional areas, for example, square, cylindrical, triangular, and hexagonal. The evolution of 3D printing technology in recent years has fundamentally increased the design freedom for energy-absorbing structures with diverse configurations, consequently broadening the scope of design possibilities. [10-14].

While various materials are used for safety-enhancing energy-absorbing structures, steel and aluminum are commonly used metals in the production of thin-walled tubes. Recently, thermoplastic materials have gained increasing importance in the industry as energy absorbers due to properties such as high energy absorption, excellent specific strength, growing environmental concerns, and sustainability for recycling. Furthermore, thermoplastic polymers have become notable as energy absorbers in the automotive industry due to their lower production cost compared to metals and the weight reduction opportunity they provide, leading to fuel efficiency, as well as their easier production. Various studies are available in the literature on this subject to improve energy absorption and crashworthiness performance. For instance, Wang et al. [15] experimentally investigated the crashworthiness behavior of multi-cell filled thin-walled hexagonal structures, fabricated using 3D printing with carbon-fiber-reinforced polyamide and featuring varying internal filling geometries and densities, under both static and dynamic loading. The study revealed that filling density and geometry substantially affect energy absorption and crushing efficiency, which further emphasized the superior performance of the proposed structures when compared to conventional designs found in the literature. The quasi-static crashworthiness of thin-walled multi-cell structures was analyzed by Hidayat et al. [16] concerning 3D printing parameters, dimensions, and filament material, ultimately determining optimal combinations for CFE and SEA. Jiang et al. [17] explored the crashworthiness of 3D-printed origami tubes with varying thickness and printing angles, demonstrating enhanced specific energy absorption in variable thickness designs and pinpointing optimal parameters for better energy absorption using experimental and finite element methods. Moreover, Meram and Sözen [18] conducted an experimental study to analyze the effect of FDM printing parameters (filling rate and pattern, specifically honeycomb, square, and concentric) on the low-velocity impact response and energy absorption of thin-walled tubes, concluding that the square pattern with a 50% filling rate was the most effective in absorbing impact energy. Abd El-Halim et al. [19] examined computationally and experimentally the crashworthiness of 3D-printed circular PLA tubes with circular hole cuts under quasi-static axial compression, employing the Taguchi method to optimize design parameters (hole diameter, number, and position) for minimizing initial PCF and maximizing absorbed energy.

Aside from the thin-walled tube configurations highlighted above, tubes with intentionally added windows or perforations on their outer walls are likewise recognized as promising energy-absorbing structures. In the literature, it has been introduced that windowed thin-walled tubes provide stabilization during the crushing process, enable the prediction and control of the collapse mode, and are a way to reduce the initial peak force [20-24]. However, studies investigating the crash behavior and energy absorption capabilities of windowed or perforated tubes have received limited attention. Therefore, this study aims to investigate the impact performance of thin-walled square tubes produced from PLA material using the Fused Deposition Modelling (FDM) process. This research seeks to determine how windows of varying numbers and sizes affect the resulting unique deformation modes of the structures under impact, as well as the ideal balance between energy absorption performance and PCF. Within this scope, quasi-static compression tests were applied to the manufactured specimens. Parameters such as different numbers of windows (4 and 5), different window

lengths (8 mm and 10 mm), and different window widths (10 mm and 12 mm) along the tube were applied to the walls of the thin-walled square tubes. By examining these factors, the energy absorption performance and crashworthiness of the thin-walled tubes were evaluated by considering crash indices such as total EA, SEA, PCF, MCF, and CFE.

2. Materials and Methods

2.1. Material properties

In this study, to investigate the effect of varying window sizes on the energy absorption of thin-walled tubes, PLA filament rolls with a diameter of 1.75 mm were procured from eSUN (Shenzhen, China). PLA was selected due to its advantages, including sustainability through renewability, environmental friendliness, cost-effectiveness for various applications, and biodegradability. PLA material is highly suitable for precision engineering applications, ensuring dimensional stability during 3D printing. Additionally, it exhibits favorable mechanical properties under compressive loading. Therefore, PLA material was chosen in this study to compare the crash performance of windowed tubes with varying window size parameters. Tensile tests were conducted on PLA specimens in accordance with ASTM D638 standards to determine the material's properties, which are listed in Table 1 (Figure 1). Using a Shimadzu Universal Test Machine, tensile tests were performed on the specimens at a speed of 2 mm/min with a 5 kN load cell.

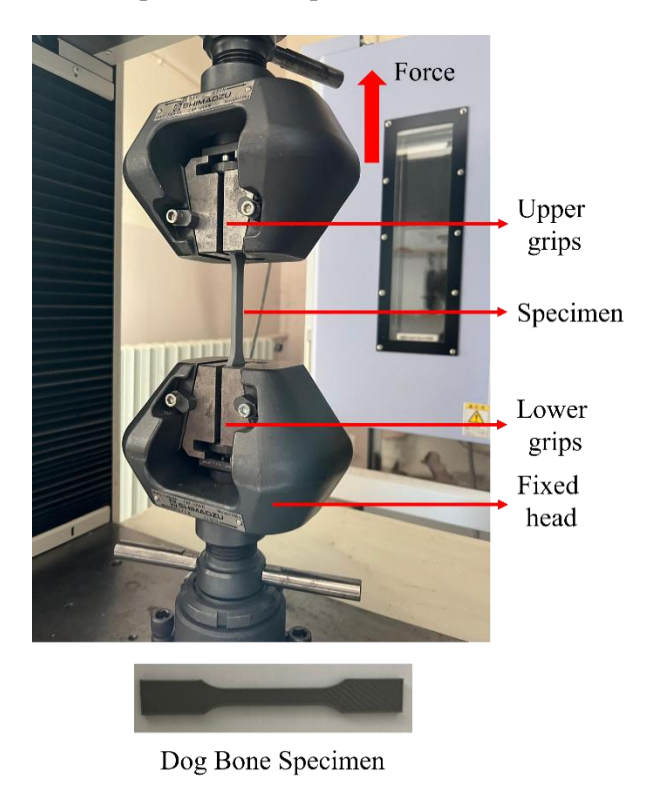


Figure 1. Tensile test and 3D printed PLA dog-bone

Table 1. Mechanical characteristics of PLA

Young's modulus (E)	Ultimate strength	Strain at max stress	Poisson's ratio	Density
2.4 GPa	51.2 MPa	0.024	0.35	1.24 g/cm ³

2.2. Geometrical design and specimen preparation

Print speed

The selection of design parameters plays a decisive role in shaping both the research approach and its findings. In this study, six design variables were carefully defined. Since no standard geometries exist for crashworthy structures [20, 25-26], the ranges were determined through experimental trials and expert knowledge to avoid any issues during fabrication.

The thin-walled tubes were fabricated from PLA material using a 3D printer employing the Fused Deposition Modeling (FDM) method. CAD models of the square cross-section thin-walled tubes were created using SolidWorks® 2018, a software developed by Dassault Systèmes - SolidWorks Corporation, and exported in Stereo Lithography (STL) format. Subsequently, Ultimaker Cura 5.4, a computer-aided manufacturing (CAM) software, was utilized to convert the models into G-code, which is essential for manufacturing on the FDM machine. The 1.75 mm diameter filament was heated in a mold, subjected to feeding by a cylindrical mechanism, and extruded through a 0.4 mm diameter nozzle. The room temperature was maintained at approximately 25°C throughout the printing process. This precise environmental control helps mitigate common printing defects like warping, inadequate build plate adhesion, inter-layer delamination, and bending, which could otherwise negatively impact part quality. The printing parameters, derived from filament vendor recommendations and previously conducted studies, are listed in Table 2.

Figure 2 illustrates the models of the four different windowed thin-walled tubes used in this study. Here, the height of the thin-walled tubes is denoted by H, the width by d, the thickness by t, the window heights by l, and the window widths by w. Table 3 provides the specifications of the fabricated thin-walled tubes.

Parameter	Unit	PLA
Printing temperature	[°C]	205
Substrate temperature	[°C]	60
Diameter of nozzle	[mm]	0.4
Thickness of layer	[mm]	0.2
Infill density	[%]	100

Table 2. 3D printing parameters of PLA

Table 3. Geometrical parameters of square thin-walled windowed tubes

[mm/s]

50

Windowed tubes	H (mm)	d (mm)	t(mm)	l (mm)	w (mm)
4W-1	90	35	2	8	12
4W-2	90	35	2	10	10
4W-3	90	35	2	10	12
5W-1	90	35	2	8	12
5W-2	90	35	2	10	10
5W-3	90	35	2	10	12

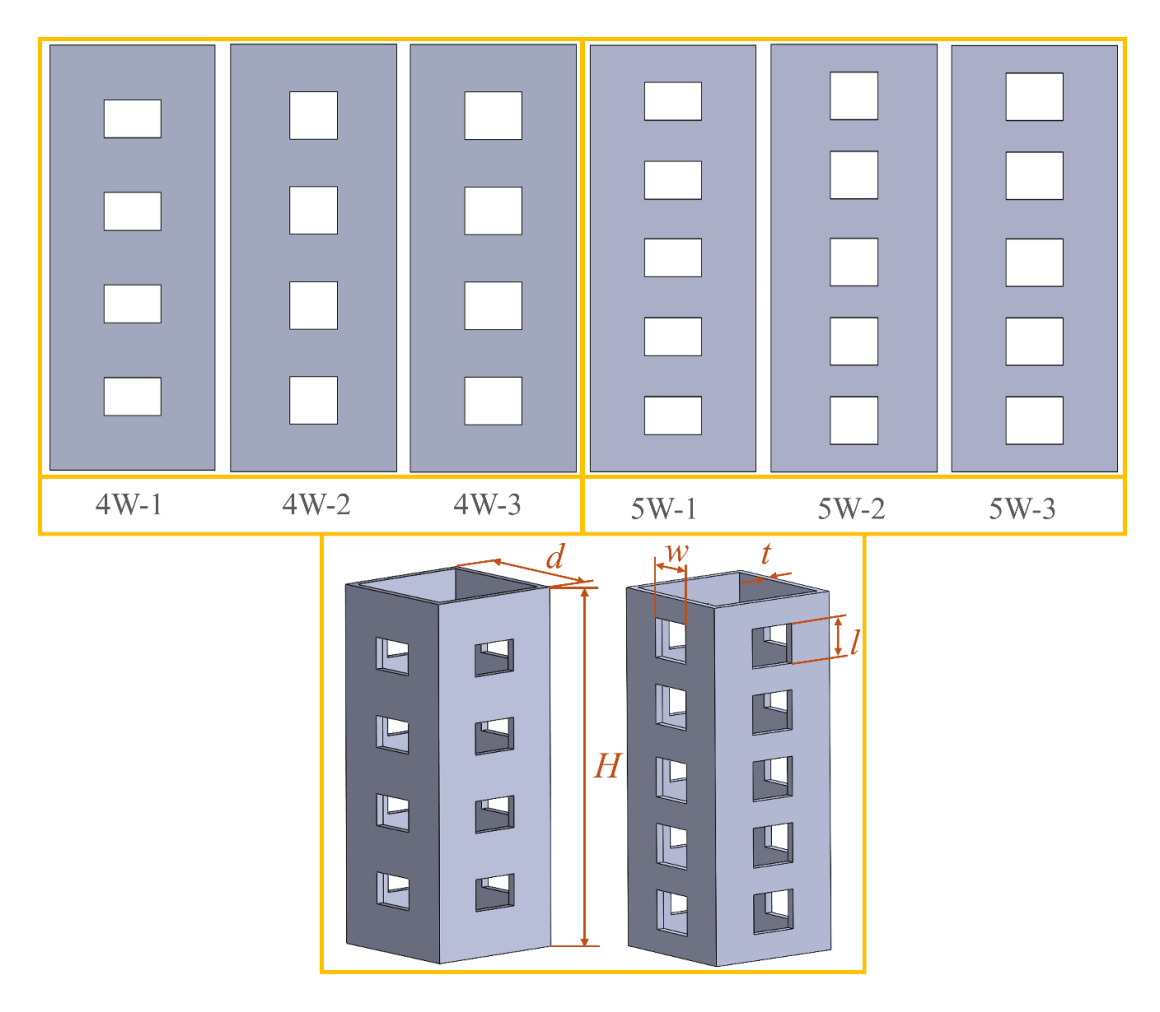


Figure 2. Windowed thin-walled tubes models

2.3. Quasi-static experimental tests

The quasi-static axial compression tests were carried out by means of a 100 kN capacity Shimadzu Universal Testing Machine. The experimental setup was conducted at room temperature and is illustrated in Figure 3. The windowed square cross-section thin-walled tubes were placed between two rigid metal plates, and the specimens were compressed using the test machine fixtures. Upon ensuring proper compression alignment, the test was initiated. In the test system, the lower fixture was fixed, while a downward displacement rate of 2 mm/min was applied by the upper fixture. During the compression, displacement was controlled, achieving a final displacement of 60 mm, corresponding to 2/3 of the initial tube height [15, 25-26]. The testing machine automatically recorded the displacement and crushing force data. Additionally, a real-time camera was used to capture the deformation behaviors of the windowed tubes under axial quasi-static loading. To ensure the reliability of the results, each specimen was subjected to the test three times, and the averages were taken to more accurately evaluate the crashworthiness behavior and energy absorption performance of the tubes.

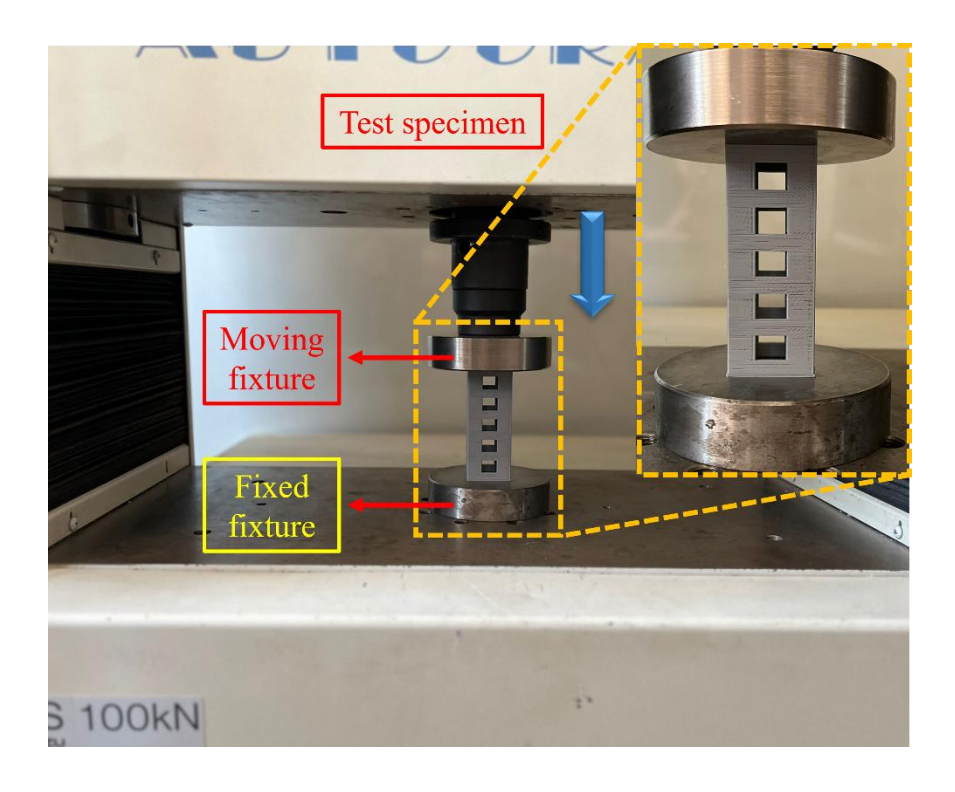


Figure 3. Experimental setup for quasi-static axial compression tests

2.4. Energy absorption parameters

The crashworthiness behavior of the thin-walled windowed square tubes is evaluated using the following crash criteria: EA, PCF, SEA, CFE, and MCF. EA, representing the energy absorbed by the thin-walled tubes during the axial compression test, is calculated as the area under the force-displacement curve. Meanwhile, SEA quantifies the energy absorbed per unit mass of the thin-walled tubes. PCF is the highest force value initially generated during the compression process. MCF is defined as the average force sustained throughout the compression process, calculated by dividing the total absorbed energy by the effective displacement. [27, 29]. The CFE value is obtained by dividing the MCF value by the PCF value and is used to assess the actual crash performance of the windowed tubes. Here, it is desired that the PCF value be low to minimize passenger safety and vehicle damage. SEA value is an important criterion for understanding the energy absorption capacity [30-31]. A high MCF value indicates that the energy-absorbing structure has good resistance to impact. Additionally, the CFE value is an important criterion for the efficiency of energy-absorbing structures, and a high CFE value indicates the structures' high impact resistance [32-33]. EA, SEA, MCF, and CFE are expressed by the following equations:

$$EA = \int_{0}^{d} F(x) dx \tag{1}$$

$$S E A = \frac{E A}{m} \tag{2}$$

$$M C F = \frac{E A}{d}$$
 (3)

$$C F E = \frac{M C F}{P C F} \tag{4}$$

where F(x), d, and m represent the instantaneous crushing force at displacement x, the axial displacement, and the mass of the thin-walled tube, respectively.

3. Results and Discussion

This section examines the crashworthiness performance of four-windowed and five-windowed thin-walled tubes with square cross-section under quasi-static compression loading. The crash performance of the windowed tubes was assessed and compared using SEA, PCF and CFE responses. Figures 4-7 display the force-displacement curves, deformation modes for each tube, EA/SEA and PCF/MCF/CFE responses, respectively. All fabricated thin-walled tubes underwent quasi-static compression tests using a universal testing machine at a crosshead speed of 2 mm/min. Force-displacement data, recorded at a frequency of 20 data points per second, was acquired from the testing machine to facilitate the comparison of the energy absorption performance of the windowed square tubes. Figure 4 demonstrates representative forcedisplacement curves for the thin-walled square tubes with varying window numbers and sizes. Consistent with common presentations in the literature, the force-displacement curves of energy-absorbing structures can be divided into three primary regions: (a) elastic, (b) plateau, and (c) densification. The elastic region is characterized by the absence of plastic deformation. The initial response of the thin-walled tubes is elastic deformation, continuing until a critical threshold is exceeded, leading to the onset of plastic deformation via yielding, fracture, buckling, or creep. Subsequently, the plastic region exhibits a rapid decrease in force, transitioning to a relatively stable force plateau as displacement increases due to internal core crushing, with the extent of the plateau directly correlating with energy absorption capacity. Across all tested thin-walled windowed tubes, the initial PCF was consistently identified within the displacement range of 1 mm to 10 mm. The highest IPF values recorded were 1.378 kN for specimen 4W-1 and 1.340 kN for specimen 5W-1, while the lowest IPF values measured were 1.334 kN for specimen 4W-3 and 1.291 kN for specimen 5W-3. A trend of decreasing IPF values with increasing window area was evident, which aligns with findings reported in the literature [21]. Following the attainment of the IPF, all thin-walled tubes transitioned into the post-crushing region, where the force values oscillated around the MCF. The thin-walled windowed tubes, in all cases, displayed inconsistent PCF values between the initial peak and the onset of densification. After the windowed thin-walled tubes had fully crushed, the force values began to ascend, signifying entry into the densification region, a stage that reached approximately 60% of the original height of the thin-walled tubes in this investigation. Figure 5 illustrates the deformation modes of windowed square tubes with 4 and 5 windows at various displacements, as observed during quasi-static compression tests. Figure 5 reveals that cracks initially appeared from the central window for the 5-window tube, whereas for the 4-window tube, they emerged from the bottom window. As the crushing event progressed, these cracks in the 4-window tube were followed by folding, while the 5-window tube exhibited local buckling. The deformation mode of the 5W-1 tube, shown in Figure 5, was observed to be local buckling. In Figure 4, it can be seen that the plateau region of the force-displacement curve proceeds smoothly without noticeable fluctuations, indicating good consistency. On the other hand, the deformation mode of the 4W-1 tube progressed in a folding manner in Figure 4, which supports the appearance of peaks in the force—displacement curve.

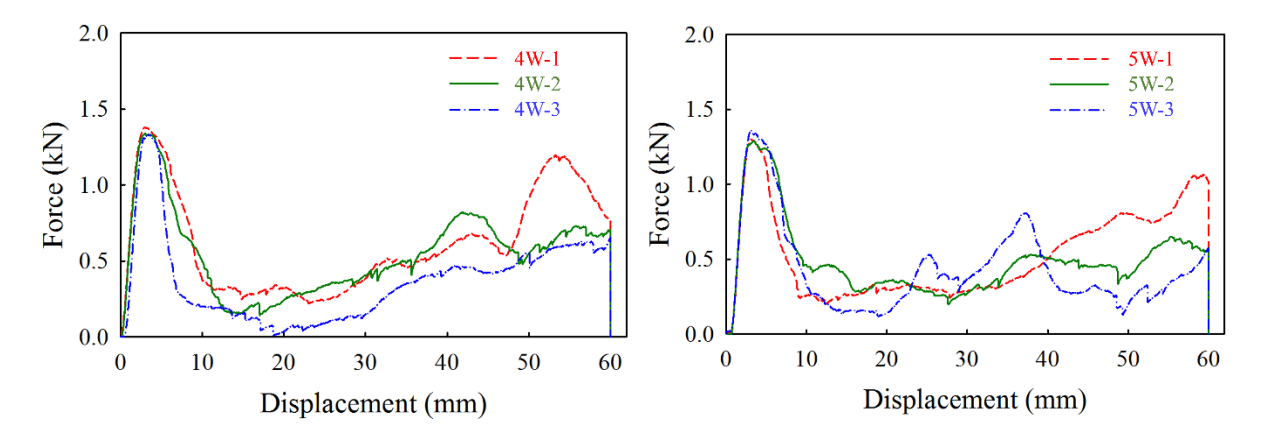


Figure 4. Force-displacement graphs of four and five windowed thin-walled tubes

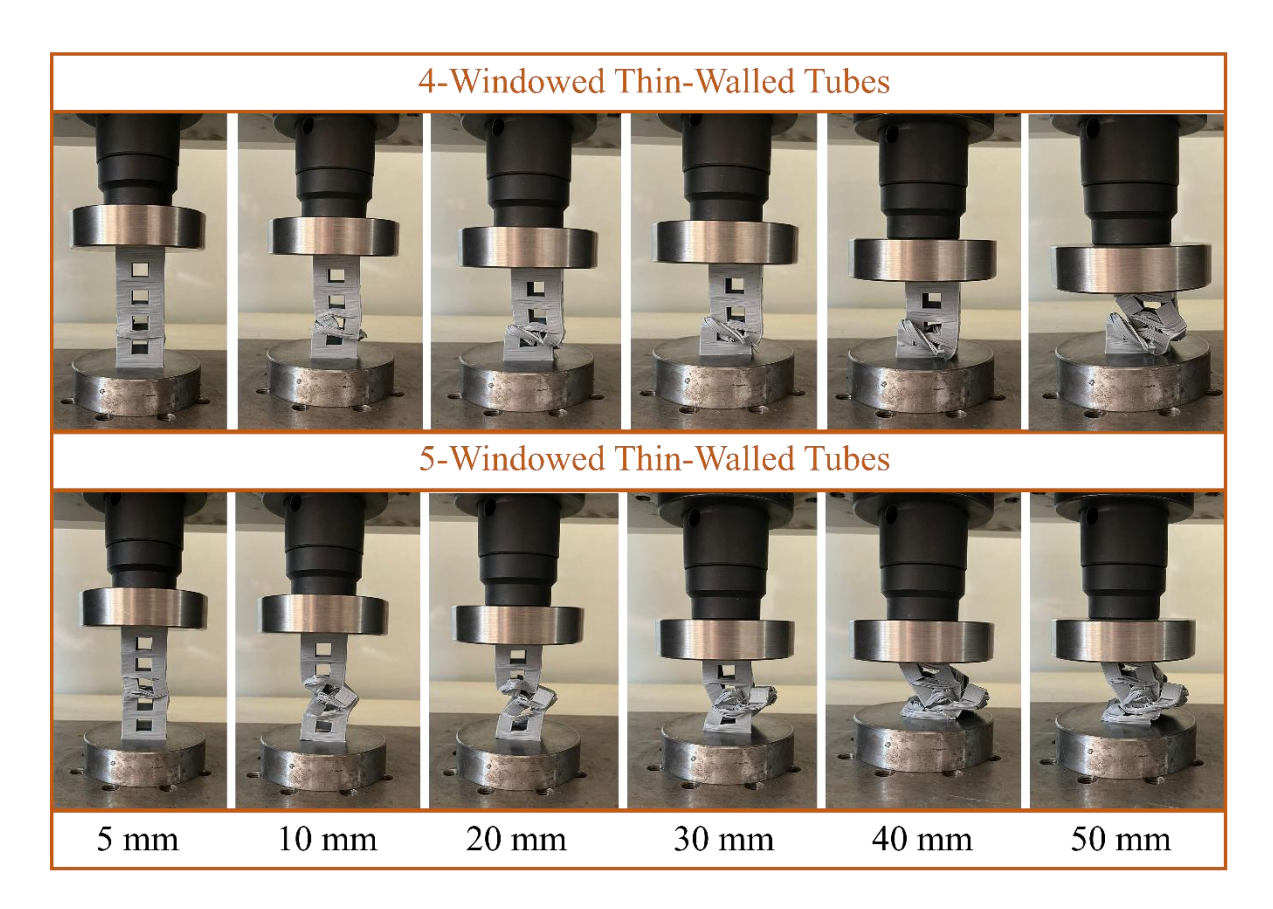


Figure 5. Deformations of tested windowed square thin-walled tubes with varying window configurations

To investigate the correlation of window numbers and dimensions on the energy absorption characteristics of thin-walled tubes, a comparative analysis of energy absorption parameters is provided in Figures 6-7. Figure 6 specifically details the EA and SEA values for windowed thin-walled square tubes. The experimental results revealed that the 4W-1 and 5W-1 specimens exhibited the highest EA values, quantified as 36.35 J and 31.31 J, respectively. Conversely, the 4W-3 and 5W-3 specimens demonstrated the lowest EA values, measured at 21.43 J and 25.49 J, respectively. This notable variation in EA capacity underscores the critical influence of window dimensions on the performance characteristics of thin-walled tubular structures. In contrast, when comparing the EA values of thin-walled tubes with varying numbers of windows but identical dimensions, observations indicated that the EA value decreased as the number of windows increased. For instance, the EA values of the 4W-1, 4W-2, and 4W-3 samples were approximately 16%, 11%, and 2.7% higher, respectively, than the EA values of the 5W-1, 5W-2, and 5W-3 samples. The findings unequivocally illustrate the impact of augmented window quantity on the EA performance of windowed tubular structures. An examination of the SEA plots for the windowed tubes reveals an inverse correlation between both window size and number and the SEA value. This phenomenon can be attributed to a more pronounced reduction in the average crushing load and energy absorption. Furthermore, an increased number of windows may disrupt the collapse mode, diminish the available material for plastic deformation, and consequently, reduce the extent of the plastic zones. For example, the experimental data indicate that the 4W-1 specimen attained a SEA value of approximately 2.15 J/g, representing enhancements of approximately 18% and 70% relative to the SEA values observed for the 4W-2 and 4W-3 specimens, respectively. Similarly, the 5W-1 specimen exhibited an SEA value of approximately 1.91 J/g, surpassing the SEA values of the 5W-2 and 5W-3 specimens by approximately 12% and 16%, respectively.

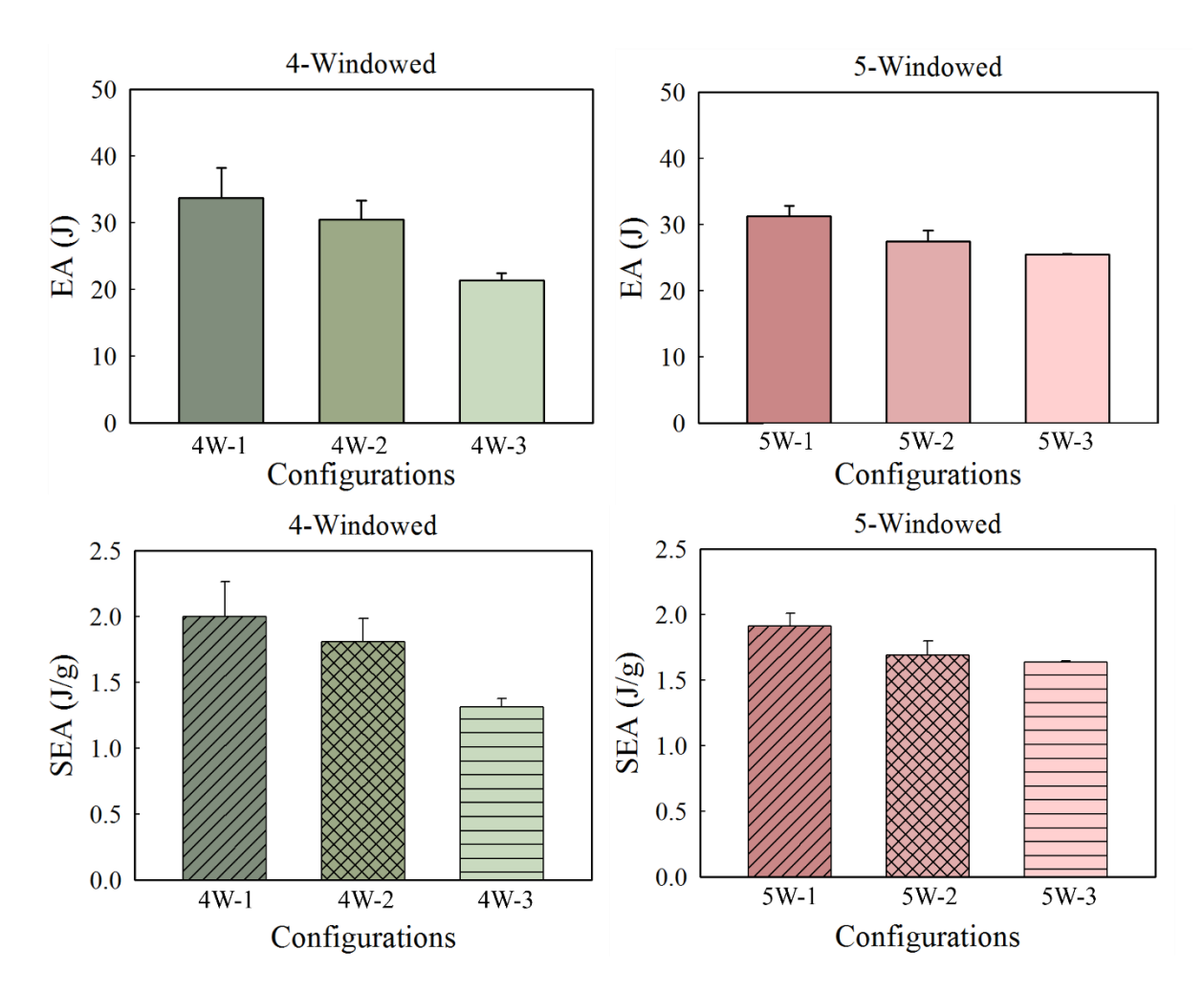


Figure 6. EA and SEA values of windowed tubes under quasi-static compression loading

Figure 7 presents a comparative analysis of the PCF, MCF and CFE as metrics characterizing the crash performance of windowed tubular structures incorporating windows. The data reveal a trend of decreasing PCF values with the augmentation of window dimensions for both the four-windowed and five-windowed tube configurations. This phenomenon can be attributed to the reduced material volume within the deformation regions as the window size increases, thereby necessitating a diminished initial force to trigger the crushing mechanism. Furthermore, the presence of windows induces local buckling along the sides of the windowed tubes, thereby also contributing to a lower initial PCF. Similarly, thin-walled tubes with windows of the same size but a greater number also exhibit a lower initial crushing force. The reason for this reduction can again be attributed to the fact that thin-walled tubes with a higher number of windows possess less material. For instance, the 4W-3 thin-walled tube specimen exhibits approximately 3.2% and 2.5% lower PCF values compared to the 4W-1 and 4W-2 specimens, respectively, while the 5W-3 thin-walled tube specimen demonstrates approximately 3.8% and 1.6% lower PCF values compared to the 5W-1 and 5W-2 specimens, respectively. Furthermore, the 5W-1 thin-walled tube specimen has approximately 2.8% lower PCF value compared to the 4W-1 specimen. A reduction in the MCF is observed with both the augmentation of the number of windows and the expansion of the window dimensions. Given that the MCF value is assessed across a consistent deformation interval, its behavior mirrors the trends observed in the energy absorption characteristics. This could be attributed to the fact that more windows relatively disrupt the collapse mode and subsequently reduce the plastic regions. The CFE is valued as a notable parameter, quantifying the effectiveness of a material or structural design in the management and distribution of forces generated during impact scenarios. The number and size of windows in thin-walled tubes play a considerably influential role in determining the CFE. The reason for a higher CFE is the significant increase in the MCF rather than a decrease in the initial peak crushing load. An increased number and size of windows lead to a reduction in the CFE value. This phenomenon is attributable to larger window sizes and a greater number of windows relatively disrupt the collapse mode and subsequently reduce the plastic deformation areas. As

illustrated in Figure 7, the 4W-1 specimen demonstrated peak CFE with a recorded value of 0.440, signifying a substantially superior capacity for the management and distribution of crash forces relative to the other tested configurations. Moreover, the CFE of the 4W-1 specimen surpassed those of the 4W-2 and 4W-3 specimens by approximately 19% and 28%, respectively, and exhibited an approximately 13% higher CFE compared to the 5W-1 specimen, a five-windowed thin-walled tube with equivalent dimensions. When comparing the thin-walled tubes with five windows, the CFE of 5W-1 was approximately 11% and 18% higher than those of 5W-2 and 5W-3, respectively.

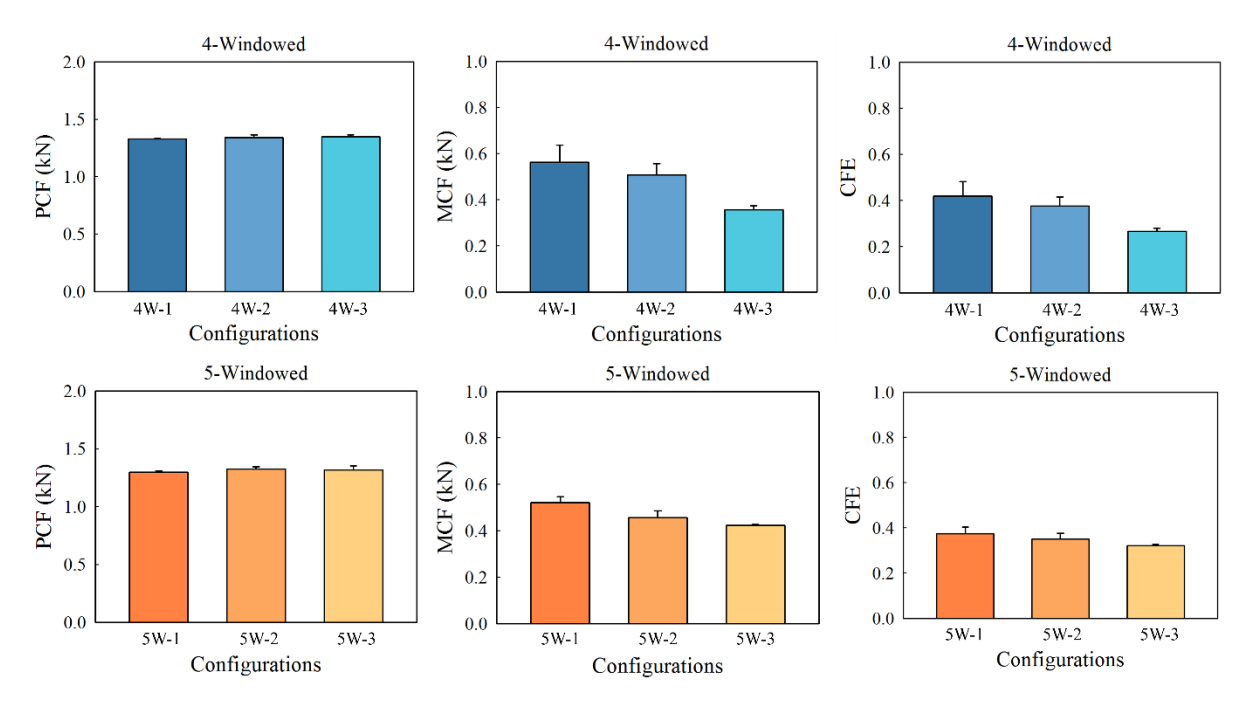


Figure 7. PCF, MCF and CFE values of windowed tubes under quasi-static compression loading

4. Conclusion

The primary objective of this study was to investigate the crashworthiness and energy absorption performance of 3D-printed thin-walled square tubes manufactured from PLA and featuring windows of varying dimensions, subjected to quasi-static axial compression. To achieve this, different parameters, specifically the window width, window length, and number of windows, were systematically varied and experimentally analyzed. Experimental tests were conducted by applying quasi-static axial compression loads to the windowed tubes at a displacement rate of 2 mm/min. Force-displacement data for the windowed tubes were meticulously recorded. To evaluate the crashworthiness and energy absorption behavior, key parameters such as PCF, EA, SEA, MCF and CFE were utilized and calculated. Firstly, PLA offers a highly sustainable alternative to conventional polymers in crashworthy designs, as its renewable origins and potential biodegradability align well with contemporary eco-conscious manufacturing and design principles. The results revealed that the PCF for all windowed thin-walled tubes consistently occurred within the early displacement range of 1-10 mm, with specimens 4W-1 and 5W-1 exhibiting the highest PCF values and 4W-3 and 5W-3 showing the lowest. A direct inverse correlation was observed between window dimensions and energy absorption, where larger windows consistently resulted in diminished energy absorption. Furthermore, specimens with fewer windows (e.g., 4W-1 and 4W-2 series) demonstrated superior energy absorption capabilities compared to their counterparts with a greater number of windows (e.g., 5W series). Additionally, the increasing number of windows was found to adversely affect the collapse mode and limit plastic deformation, consequently leading to reduced SEA. In contrast, specimens with fewer windows, exemplified by 4W-1 (approx. 2.15 J/g), exhibited superior SEA, showing an 18% to 70% improvement over 4W-2 and 4W-3, respectively. Among the investigated structures, the 4W-1 configuration demonstrated the best performance and can therefore be highlighted as the optimum design. This study also revealed that increasing both the number and size of windows significantly diminished the CFE, a reduction attributed to the disruption of the collapse mode and the decrease in plastic deformation areas. Correspondingly, specimen

4W-1 exhibited an optimal CFE of 0.440, underscoring its superior capability in managing and distributing impact forces among the tested configurations. Subsequent studies are warranted to ascertain the effect of differing window geometries on energy absorption performance, diverging from the rectangular profiles considered herein.

5. Acknowledgement

During the preparation of this work, the author used artificial intelligence-assisted technology tools OpenAI ChatGPT and Google Gemini, in order to improve language and readability, with caution. After using this tool, the author reviewed and edited the content as needed and takes full responsibility for the content of the publication. The scientific content, analyses, results, and discussions are entirely the author's own work, conducted in accordance with scientific research methods and academic ethical principles.

6. Author Contribution Statement

Merve Tunay: Conceptualization, Investigation, Methodology, Resources, Visualization, Writing-Original Draft, Writing-Review&Editing

7. Ethics Committee Approval and Conflict of Interest

There is no need for an ethics committee approval in the prepared article. There is no conflict of interest with any person/institution in the prepared article.

8. Ethical Statement Regarding the Use of Artificial Intelligence

No artificial intelligence-based tools or applications were used in the preparation of this study. The entire content of the study was produced by the author in accordance with scientific research methods and academic ethical principles.

9. References

- [1] Z. Ghahremanzadeh, and S. Pirmohammad, "Crashworthiness performance of square, pentagonal, and hexagonal thin-walled structures with a new sectional design," Mech. Adv. Mater. Struct., vol. 30, no. 12, pp. 2353–2370, 2023.
- [2] H. Mohammadi, Z. Ahmad, M. Petrů, S.A. Mazlan, M.A.F. Johari, H. Hatami, and S.S.R. Koloor, "An insight from nature: Honeycomb pattern in advanced structural design for impact energy absorption," J. Mater. Res. Technol., Jan. 2023.
- [3] X. Zuo, C. Guo, W. Chen, Y. Wang, J. Zhao, and H. Lv, "Influence of loading rate and temperature on the energy absorption of 3D-printed polymeric origami tubes under quasi-static loading," Polymers (Basel), vol. 14, no. 18, Sep. 2022.
- [4] M. Capretti, G. Del Bianco, V. Giammaria, and S. Boria, "Natural fibre and hybrid composite thinwalled structures for automotive crashworthiness: A review," Materials, vol. 17, no. 10, May 2024.
- [5] M. Koloushani, M. R. Forouzan, and M. R. Niroomand, "On the crashworthiness performance of thin-walled circular tubes: Effect of diameter and thickness," Mech. Adv. Mater. Struct., 2023.
- [6] K. Memane, A. Mashalkar, and P. Kumar, "A review thin-wall-tube energy-absorbing structure: Crash-box," in J. Phys. Conf. Ser., 2023.
- [7] W. Li, Y. Luo, M. Li, F. Sun, and H. Fan, "A more weight-efficient hierarchical hexagonal multicell tubular absorber," Int. J. Mech. Sci., vol. 140, pp. 241–249, 2018.
- [8] S. Vyavahare, and S. Kumar, "Numerical and experimental investigation of FDM fabricated reentrant auxetic structures of ABS and PLA materials under compressive loading," Rapid Prototyp. J., vol. 27, no. 2, pp. 223–244, 2021.
- [9] M. Tunay, "Bending behavior of 3D printed sandwich structures with different core geometries and thermal aging durations," Thin-Walled Struct., vol. 194, p. 111329, 2024.
- [10] S. A. A. Alaziz, M. A. Hassan, and M. A. A. El-Baky, "Crashworthiness characteristics of bio-inspired 3D-printed tubes: A lesson from the environment," Fibers Polym., Oct. 2024.
- [11] C. Tao, X. Zhou, Z. Liu, X. Liang, W. Zhou, and H. Li, "Crashworthiness study of 3D printed lattice reinforced thin-walled tube hybrid structures," Materials, vol. 16, no. 5, Mar. 2023.
- [12] M. Tunay, and A. Bardakci, "A study of crashworthiness performance in thin-walled multi-cell tubes 3D-printed from different polymers," J. Appl. Polym. Sci., Dec. 2024.
- [13] A. Sadooghi, S. J. Hashemi, S. Mirzamohammadi, F. Rahmani, and K. Rahmani, "Enhancing compressive and crush performance of 3D-printed ABS thin-walled tubes through glass fiber reinforcement and polyurethane foam infusion," Int. J. Polym. Sci., vol. 2025, no. 1, 2025.
- [14] C. W. Isaac, and F. Duddeck, "Current trends in additively manufactured (3D printed) energy absorbing structures for crashworthiness application a review," Int. J. Crashworthiness, 2022.
- [15] K. Wang, Y. Liu, J. Wang, J. Xiang, S. Yao, and Y. Peng, "On crashworthiness behaviors of 3D printed multi-cell filled thin-walled structures," Eng. Struct., vol. 254, p. 113907, 2022.
- [16] D. Hidayat, J. Istiyanto, D. A. Sumarsono, F. Kurniawan, and R. Ardiansyah, "Investigation on the crashworthiness performance of thin-walled multi-cell PLA 3D-printed tubes: A multi-parameter analysis," Designs (Basel), vol. 7, no. 108, 2023.
- [17] Z. Jiang, J. Zhao, W. Chen, and H. Lv, "Experimental and numerical crashworthiness investigation of 3D printing carbon fiber reinforced nylon origami tubes," Polym. Compos., vol. 45, no. 4, pp. 3296–3314, Mar. 2024.
- [18] A. Meram, and B. Sözen, "Experimental investigation on the effect of printing parameters on the impact response of thin-walled tubes produced by additive manufacturing method," Int. J. Crashworthiness, vol. 28, no. 1, pp. 32–45, 2023.
- [19] M. F. Abd El-Halim, M. M. Awd Allah, A. S. Almuflih, and M. A. Abd El-Baky, "Axial crashworthiness characterization of bio-inspired 3D-printed gyroid structure tubes: Cutouts effect," Fibers Polym., 2024.
- [20] M. F. Abd El-Halim, M. M. Awd Allah, M. A. Abbas, A. A. Mousa, S. F. Mahmoud, and M. A. Abd El-Baky, "Energy absorption performance of 3D-printed windowed structures under quasi-static axial loading condition," Fibers Polym., Jan. 2024.
- [21] J. Song, and F. Guo, "A comparative study on the windowed and multi-cell square tubes under axial and oblique loading," Thin-Walled Struct., vol. 66, pp. 9–14, 2013.

- [22] J. Song, Y. Chen, and G. Lu, "Light-weight thin-walled structures with patterned windows under axial crushing," Int. J. Mech. Sci., vol. 66, pp. 239–248, Jan. 2013.
- [23] H. Nikkhah, A. Baroutaji, and A. G. Olabi, "Crashworthiness design and optimisation of windowed tubes under axial impact loading," Thin-Walled Struct., vol. 142, pp. 132–148, Sep. 2019.
- [24] C. Zhou, S. Ming, C. Xia, B. Wang, X. Bi, P. Hao, and M. Ren, "The energy absorption of rectangular and slotted windowed tubes under axial crushing," Int. J. Mech. Sci., vol. 141, pp. 89–100, Jun. 2018.
- [25] P. Feraboli, B. Wade, F. Deleo, and M. Rassaian, "Crush energy absorption of composite channel section specimens," Compos. Part A Appl. Sci. Manuf., vol. 40, no. 8, pp. 1248–1256, 2009.
- [26] F. R. Deleo, and P. Feraboli, "Crashworthiness energy absorption of carbon fiber composites: Experiment and simulation," Ph.D. dissertation, Univ. of Washington, 2011.
- [27] K. Wang, G. Sun, J. Wang, S. Yao, M. Baghani, and Y. Peng, "Reversible energy absorbing behaviors of shape-memory thin-walled structures," Eng. Struct., vol. 279, p. 115626, 2023.
- [28] J. Wang, Y. Liu, K. Wang, S. Yao, Y. Peng, Y. Rao, S. Ahzi, "Progressive collapse behaviors and mechanisms of 3D printed thin-walled composite structures under multi-conditional loading," Thin-Walled Struct., vol. 171, p. 108810, 2022.
- [29] C. Gong, Z. Bai, Y. Wang, and L. Zhang, "On the crashworthiness performance of novel hierarchical multi-cell tubes under axial loading," Int. J. Mech. Sci., vol. 206, p. 106599, 2021.
- [30] H. S. Googarchin, S. Sadeghi, and A. Keshavarzi, "Numerical analysis of bio-inspired foam-filled multi-cell tapered tubes for energy absorption," Mech. Based Des. Struct. Mach., pp. 1–28, 2025.
- [31] M. M. Awd Allah, D. A. Hegazy, H. Alshahrani, T. A. Sebaey, and M. A. Abd El-Baky, "Exploring the effect of nanoclay addition on energy absorption capability of laterally loaded glass/epoxy composite tubes," Polym. Compos., 2023.
- [32] A. Keshavarzi, and H. S. Googarchin, "Local reinforcement of adhesively bonded square shape aluminum energy absorber with CFRP under quasi-static axial loading: An experimental and numerical study," Int. J. Adhes. Adhes., vol. 135, Dec. 2024.
- [33] G. Zhu, J. Liao, G. Sun, and Q. Li, "Comparative study on metal/CFRP hybrid structures under static and dynamic loading," Int. J. Impact Eng., vol. 141, p. 103509, 2020.